



ELSEVIER

Available online at www.sciencedirect.com

SCIENCE @ DIRECT®

Optics Communications 216 (2003) 391–399

OPTICS
COMMUNICATIONS

www.elsevier.com/locate/optcom

Heterodyne frequency calibration of high resolution cesium spectra using diode lasers

Vladislav Gerginov, Carol E. Tanner*

Department of Physics, College of Science, University of Notre Dame, 225 Nieuwland Science Hall, Notre Dame, IN 46556-5670, USA

Received 2 October 2002; received in revised form 4 December 2002; accepted 9 December 2002

Abstract

We describe our system for frequency calibrating high resolution laser induced fluorescence spectra. The system utilizes two diode lasers that are spectrally narrowed with optical feedback from external resonators. One laser acts as a reference and is locked to a cesium transition with an external resonator containing a vapor cell in a Faraday filter configuration. Additional electronic feedback fixes the length of the resonator. The second laser receives its feedback from a confocal optical cavity and has the capability of scanning over several hundred megahertz. A portion of the scanning-laser output excites cesium atoms in a thermal atomic beam producing a fluorescence signal. Portions of each laser output are combined on a fast photo diode that produces a heterodyne signal. A counter reads the RF beat note between the laser frequencies and provides the frequency calibration.

© 2002 Elsevier Science B.V. All rights reserved.

PACS: 42.55.-f; 42.55.Px; 42.60.-v; 42.62.Fi; 32.70.Cs

Keywords: High resolution spectroscopy; Diode lasers; Optical feedback; Heterodyne; Laser stabilization

1. Introduction

Our motivations for constructing this laser system involve two types of spectroscopy experiments presently underway in our laboratory. These experiments involve the low-lying electronic states of Cs which are shown in Fig. 1 along with the corresponding hyperfine splittings.

The first experiment is the precise measurement of the $^{133}\text{Cs}6p^2P_{3/2}$ state hyperfine splittings. With the laser system described here, we can acquire well-calibrated fluorescence spectra from which we can determine the splittings to a precision of a few kilohertz. This is about an order of magnitude better than the most accurate previous results [1]. From measurements of these hyperfine splittings, one can determine the strength of the magnetic dipole, electric quadrupole, and magnetic octupole interactions between the nucleus and the orbital electrons [2]. When our measurements are completed, we expect the results will provide tests for theories of atomic and nuclear structure.

* Corresponding author. Tel.: +1-219-6318369; fax: +1-219-6315952.

E-mail address: carol.e.tanner.1@nd.edu (C.E. Tanner).

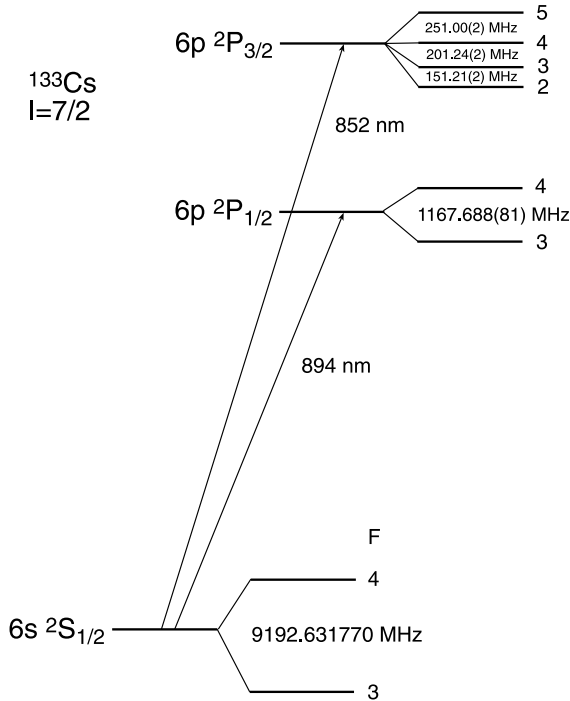


Fig. 1. Shown are the low-lying electronic states of atomic cesium with hyperfine intervals [1,14,15] and rest frame transition wavelengths.

The second type of experiment involves precision absorption spectroscopy in a cesium vapor cell. The $6s^2S_{1/2} \rightarrow 6p^2P_{3/2}$ transition amplitude is well known from precision lifetime measurements of the excited state [3,4]. Therefore, an absorption spectrum of this transition can be used to calibrate the number density of cesium atoms in a cell of known length. With known density, absolute absorption measurements of other transitions can be used to determine the corresponding transition amplitudes. The laser system described here can produce absorption spectra with greater frequency resolution and less acquisition time than in our previous absorption measurements [5].

2. Reference laser

The central component of the reference laser is a model STC LT50A-03U diode laser from Spectra Diode Labs, however other diode lasers may be

used in a similar manner. These particular lasers produce a linearly polarized output of 50 mW at 852 nm in a single longitudinal mode. The tuning characteristics are typically -19.6 GHz/K and -2.69 GHz/mA. Ref. [6] describes our methods of controlling the wavelength through temperature and current along with details of the free-running behavior of these lasers. The free-running linewidth is about 15 MHz as determined by heterodyning the laser output with that of the narrowed scanning laser described below and is larger than the 2.3(1) MHz of inhomogeneous broadening due to the transverse velocity spread of our collimated thermal beam. Because we desire to calibrate laser frequency scans with a resolution of better than 25 kHz, we chose to narrow the reference-laser spectrum with optical feedback from an external resonator.

2.1. Reference-laser optical feedback

A schematic diagram of the reference laser and external cavity is shown in Fig. 2. A similar system is described by Lee et al. [7] using a rubidium vapor cell, and by Shevy et al. [8] using a cesium vapor cell. In our system, the diode laser output is roughly collimated with a short focal length lens. The external cavity is formed between the diode laser output facet, a 50% nonpolarizing beam splitter, and a concave 99.5% reflective mirror with a 500 cm radius of curvature. The beam splitter allows 50% of the light to exit the external cavity

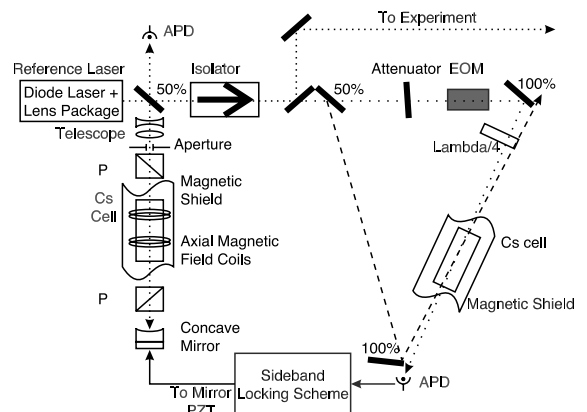


Fig. 2. Schematic of reference laser.

for use in the experiment. In the external cavity, a filter based upon the Faraday effect restricts the optical feedback to a narrow bandwidth near the cesium resonances. The Faraday filter is based on a cesium vapor cell between crossed polarizers. A pair of 10 cm diameter coils, separated by 10 cm, are placed outside the cell to produce a longitudinal magnetic field of up to 1.5 Gauss along the axis of the laser beam. Magnetic Shielding outside the coils eliminates the influence of stray fields on the cesium atoms. As the incident 20 mW laser beam propagates through the external cavity, it encounters beam expanding optics and an iris diaphragm reducing its diameter to 5 mm. After that, it passes through a linear polarizer with its axis parallel to the laser polarization, a cesium cell, a linear polarizer perpendicular to the first, and a concave retro-reflecting mirror. With a small magnetic field and the laser light tuned near resonance, the cesium vapor rotates the linear polarization. The strength of the magnetic field controls the amount of rotation and effectively the transmission of the polarizer–cell–polarizer combination. The transmission is also affected by the detuning of the laser from resonance with the greatest transmission occurring in a narrow bandwidth near each resonance. The longitudinal magnetic field and temperature are found to strongly affect the amount of rotation and the resonance bandwidth. The retro-reflecting mirror sends the transmitted light back through the narrow bandwidth filter. The returning light reaches the laser mode matched and with the same polarization as the original output. One port of the beam splitter also allows us to monitor the intensity of the optical feedback to the laser as a function of free-running laser frequency detuning. The optical feedback spectrum with the reference-laser excitation starting from $F = 4$ ground state component is shown in Fig. 3. The retro-reflecting mirror is slightly misaligned in this case, and the light transmitted through the 50% beam splitter is monitored with an avalanche photodiode (APD). One can see that the Faraday filter is open when the free-running laser frequency is in the vicinity of the cycling transition ($F = 4$ ground state component and $F' = 5$ upper state component) or one of the cross-over resonances between $F' = 5$ and

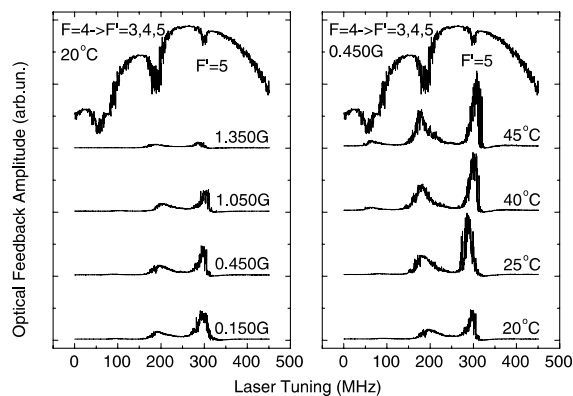


Fig. 3. Plot of reference-laser optical feedback versus laser tuning. The laser excitation starts from $F = 4$ ground state component. On the left, magnetic field dependence at room temperature (20 °C). On the right, temperature dependence at 0.45 G magnetic field. The traces are offset for convenience.

$F' = 3, 4$ upper state components. As can be seen from Fig. 3, the temperature changes significantly the amplitude of the reflected light without affecting the linewidth. The amplitude does not increase exponentially with the vapor density due to the fact that the Cs vapor in the cell becomes optically thick. On the other hand, stronger magnetic fields can alter the spectrum significantly and make $F' = 5 \rightarrow F' = 4$ cross-over resonance comparable in amplitude with the cycling transition. Additional increase of the magnetic field can even reduce the amount of reflected light. When optical locking, the magnetic field for $F = 4 \rightarrow F' = 5$ transition is kept around 300 mG, and the temperature of the cell about 20 °C. Under these conditions the amount of light returning to the laser is less than or about 1 μ W. Qualitatively, the same behavior is found when the laser starts from the other ground state component, $F = 3$, as can be seen in Fig. 4. The magnetic field required to produce the same amount of optical feedback is larger in this case due to the fact that $F = 3 \rightarrow F' = 2$ cycling transition has 5/11 times smaller transition amplitude than that of $F = 4 \rightarrow F' = 5$. The optical locking is performed at magnetic field of 800 mG. The effect of the optical feedback on the laser frequency scan when the retro-reflecting mirror is aligned can also be seen in Fig. 5. The 15 MHz wide optical feedback

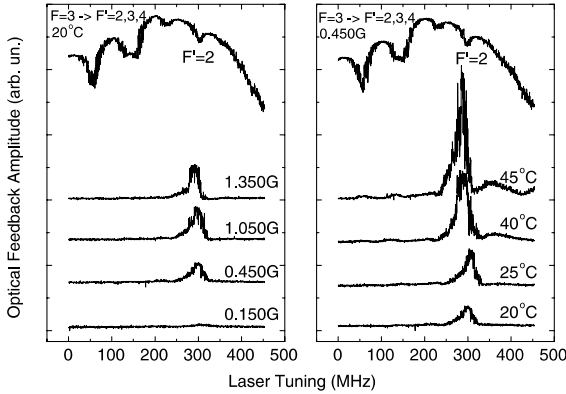


Fig. 4. Plot of reference-laser optical feedback versus laser tuning. The laser excitation starts from $F = 3$ ground state component. On the left, magnetic field dependence at room temperature. On the right, temperature dependence at 0.45 G magnetic field. The traces are offset for convenience.

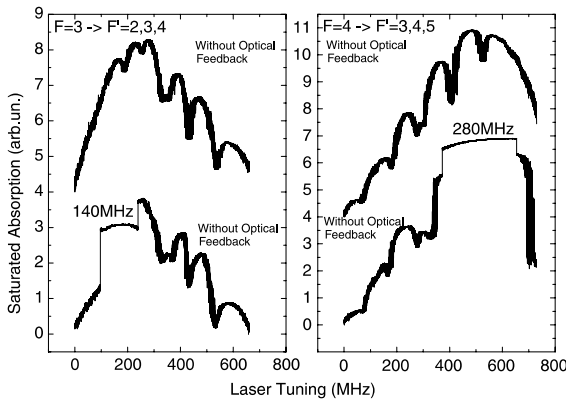


Fig. 5. Plot of reference-laser optical frequency locking versus laser tuning. On the left, laser excitation from $F = 3$ ground state component. On the right, laser excitation from $F = 4$ ground state component. The traces are offset for convenience.

(combination of the natural transition width and the free-running laser linewidth) provides a locking region of almost 150 MHz when the laser is tuned to $F = 3$ ground state component, and 280 MHz when tuned to $F = 4$ component. The strongest locking is around the cycling transitions where we usually work. With the free-running laser frequency within these regions, the diode laser locks itself to the external cavity resonance resulting in a linewidth of 50 kHz as determined by heterodyning the laser output with that of the narrowed

scanning laser described below. A single electronic feedback loop keeps the external cavity length constant and provides an hour of operation with a drift of less than 30 kHz. For longer times, a second loop would be required to keep the laser current from drifting.

2.2. Reference-laser electronic feedback

The laser and the external cavity act as coupled resonators with the laser tending to follow the resonance of the longer high finesse cavity. To prevent the laser from drifting in response to variations in length of the external cavity, we supply position feedback to retro-reflecting mirror with a tube-shaped piezo-electric transducer (PZT). The electronic feedback system is optimized for our needs of a narrow laser linewidth and a spectrally pure experimental beam. Therefore this error signal is derived from a small portion of main experimental beam using a beam splitter, leaving the main output frequency spectrum unaltered. This beam is split again into pump and probe beams before entering a saturated absorption spectrometer as shown in Fig. 2. The feedback signal is generated by adding RF sidebands to the probe beam with an electro-optic modulator (EOM) similar to the scheme introduced in [9]. An RF oscillator (not shown in Fig. 2) drives the EOM at 70 MHz. The sideband amplitude is kept around 10%. The pump beam polarization is made circular to enhance the cycling transition contrast. The probe beam is detected with a battery powered avalanche photo diode, followed by an RF operational amplifier, and the schematic is shown in Fig. 6. The high voltage required by the APD is also supplied by a 100 V battery. The high gain of the avalanche photo diode allows us to keep the power in the saturated absorption set up low to minimize line broadening effects. The RF operational amplifier allows the amplification of the signal at the EOM modulation frequency. The signal is mixed with a portion of the RF oscillator providing a laser frequency dependent error signal that is amplified and feedback to the PZT to stabilize the length of the external cavity. The saturated absorption signal and error signal are shown in Fig. 7. The 5 kHz

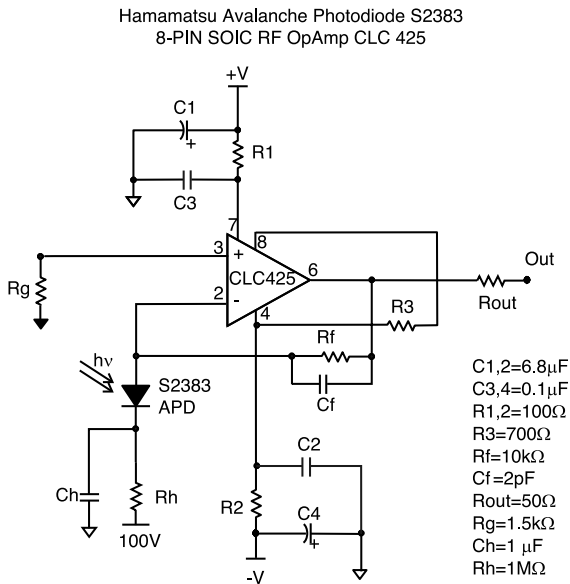


Fig. 6. Schematic of avalanche photo diode and RF operational amplifier circuit.

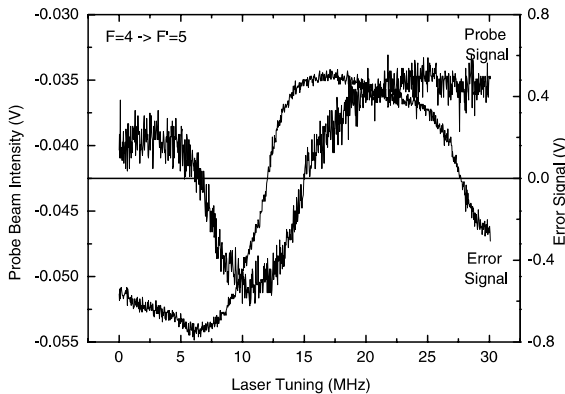


Fig. 7. Plot of electronic error signal versus the laser frequency. The laser is optically locked near $F = 4 \rightarrow F' = 5$ Cs transition and its frequency is scanned by translating the retro-reflecting mirror. The probe beam intensity in the saturated absorption spectrometer is also shown.

bandwidth of the electronic feedback is limited by the PZT.

3. Scanning laser

The central component of the scanning laser is also a model STC LT50A-03U diode laser from

Spectra Diode Labs, and it is possible that other diode lasers may be used in a similar manner. The diode laser temperature and current are controlled in the same manner as the reference laser. The free-running linewidth of the scanning laser is also about 15 MHz as determined by heterodyning the laser output with that of the narrowed reference laser. Again, because we desire to achieve a high resolution spectra, we chose to narrow the scanning-laser spectrum with optical feedback from an external confocal resonator.

3.1. Scanning-laser optical feedback

The optical feedback for the scanning laser follows the scheme investigated by Dahmani et al. [10]. A schematic diagram of our set up is shown in Fig. 8. The free-running laser has a gap in its tuning characteristics centered on the $^{133}\text{Cs } 6p^2P_{3/2}$ transition. To eliminate this problem, a small amount of optical feedback is applied to the laser by mounting a thin microscope cover slip less than a millimeter away from the laser output facet, as done in [11]. The slip is glued to a piece of low-voltage PZT. By applying a DC voltage on the PZT to translate the slip, we are able to select up to four longitudinal laser modes and to hit the Cs resonance line. A portion of the laser output is split from the main output with a 10% beam sampler and steered into a 10-cm confocal optical cavity with one mirror mounted on a PZT. The

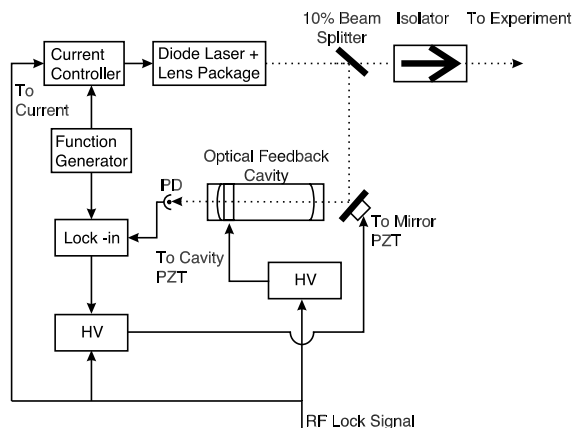


Fig. 8. Schematic of scanning laser.

initial collimating lens of the laser is positioned to provide a beam waist at the center of the confocal cavity. With the cavity tilted at small angle, resonant light is reflected back to the diode laser providing narrow bandwidth optical feedback while the specular reflection off of the input mirror is reflected away. With a steering mirror on a PZT, the phase of the optical feedback can be adjusted by changing the path length between the cavity and the laser. To keep the optical phase constant, the diode laser current is modulated at 25 kHz. The light transmitted through the cavity is detected with a photodiode and sent to a lock-in amplifier. The detuning of the phase of the optical feedback produces a dispersion signal centered on the resonance cavity transmission maximum. This signal is used to keep the phase constant. The diode laser and optical feedback system are all contained in almost entirely sealed aluminum box with a plexiglass cover to reduce acoustic vibrations from room noise that can affect the length of the external cavity. By scanning the laser current, confocal cavity, and phase mirror together, we can obtain long smooth laser frequency scans of several hundred megahertz. Fig. 9 shows the trans-

mission of a saturation spectrometer without and with resonant optical feedback from the confocal cavity along with the cavity transmission as a function of laser frequency.

3.2. Construction of confocal resonators

Our confocal cavities are assembled in a particular way. Each mirror has a reflectivity of 99.5%, a 10-cm radius of curvature, and a diameter of 1/2 in. First a pair of wires are attached to a 1/2-inch diameter PZT tube. Then the PZT tube is epoxied to the end of a 1/2-inch diameter quartz tube previously cut to the desired length and notched to allow the wire attached to the inside surface of the PZT to exit. The length of the quartz tube is cut with a glass saw so that the combined length provides the correct mirror spacing taking into account the curved surface and diameter of the mirrors. One mirror is glued to the PZT tube and the combination is mounted on a tilt stage with a single frequency tunable laser beam passing through the center of the tube and exiting the PZT mounted mirror into a photo diode. The second mirror is mounted on a good quality stage with XYZ translation and two axes of tilt and positioned at the input end of the quartz tube. While scanning the laser frequency and monitoring the cavity transmission with a photo diode, the 5 axis tilt and translation stage is used to place the second mirror in its final position relative to the quartz tube. If the length of the tube is cut properly, the edges of the second mirror should be in reasonably close contact with the end of the tube. The second mirror is then glued in place with epoxy. If the quartz tube is too long by a small amount, its length can be reduced with emery paper until a resonance condition is achieved. This construction technique results in a very rigid compact airtight cavity with a finesse of 200.

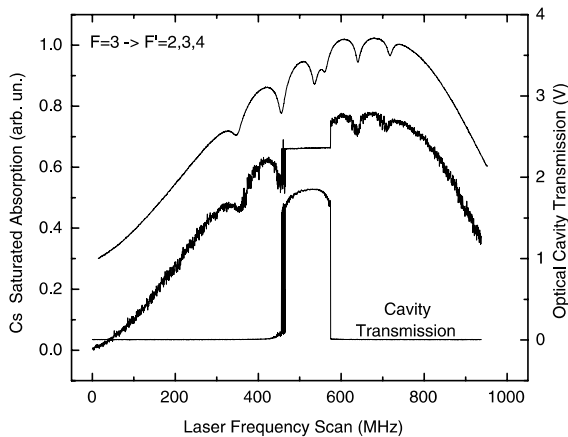


Fig. 9. Saturation spectrometer and optical feedback cavity transmission as a function of scan laser frequency. Top trace shows the saturated absorption signal when both cavity length and laser current are scanned synchronously. The second trace is the saturated absorption signal when only the laser current is scanned and not the cavity length. The bottom trace shows the cavity transmission under the same conditions. The traces are offset for convenience.

4. Heterodyning the output of two diode lasers

Our goal with this laser system is to obtain well-calibrated frequency scans of Cs fluorescence and absorption spectra. The approach we employ is similar to that of Rong et al. [12] with several

additions. A diagram of our laser system is shown in Fig. 10. A portion of scanning laser beam (90%) is sent to the thermal beam apparatus to excite Doppler-free fluorescence. Another portion of the scanning-laser beam (10%) is frequency shifted with an acousto-optical modulator. Depending on the ground state component being excited, the optical frequency is shifted up by 80 MHz ($F = 3$) or down by 80 MHz ($F = 4$) to allow nonzero frequency beat note around the cycling transitions where the reference laser is locked. This beam (1 mW) is then combined with part of the output from the reference laser (1 mW) on a beam splitter and directed to a fast photo diode. The beat note between the two lasers is monitored with an RF spectrum analyzer and highly stable RF counter. Because we desire high resolution spectra, we also lock the value of the beat note to specific values by mixing it with the output of a stable RF source that can cover a range from 250 kHz to 1 GHz. This RF source is computer-controlled to scan to and hold at specific frequency values while the computer reads the counter ($\nu_{\text{Scan Laser}} \pm \nu_{\text{AOM}} - \nu_{\text{Ref. Laser}}$) and fluorescence signal until the desired accuracy is achieved. To accomplish this offset locking, we use a frequency discriminator similar to that of Schünemann et al. [13], constructed from a band pass filter (70 MHz), RF splitter, 25 ft cable delay, and an RF mixer. Fig. 10 shows a schematic of the RF electronics. The discriminator has a dispersion-shaped transfer function plotted in Fig. 11 and provides 20 MHz wide locking interval.

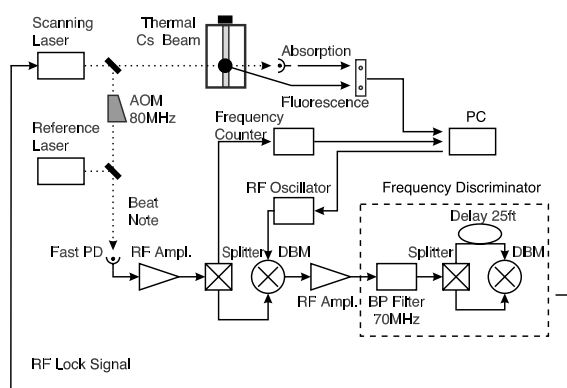


Fig. 10. Diagram of the heterodyning laser system.

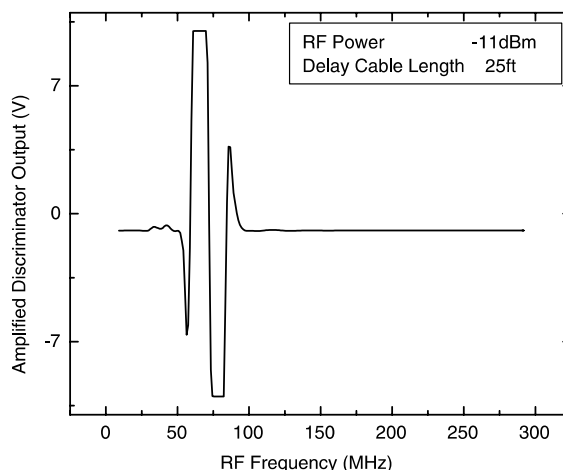


Fig. 11. Plot of RF discriminator output as a function of the applied RF frequency.

The output of the discriminator is sent to the scanning laser to lock the difference between the beat note and the RF oscillator at $70 \text{ MHz} = \nu_{\text{RF Osc.}} - (\nu_{\text{Scan Laser}} \pm \nu_{\text{AOM}} - \nu_{\text{Ref. Laser}})$. Since the reference laser is locked to a specific transition, the scanning-laser frequency is changed as the RF oscillator is being scanned.

5. Thermal atomic beam

The high resolution spectra presented here require a high current and well-collimated atomic beam. The details of our design are to be published elsewhere, however we give a brief description and the relevant experimental parameters here. The cesium oven comprises a nozzle and reservoir. The nozzle is constructed of a stainless steel vessel surrounded by heaters. Atomic cesium vapor effuses from the nozzle through an array of closely packed 21 gauge thin wall stainless steel tubes. The array has dimensions $5 \times 15 \text{ mm}$, where the longer side is parallel to the excitation laser direction of propagation. The cesium reservoir is constructed of commercial stainless steel vacuum components with knife edge seals. A metal seal bellows valve between the reservoir and the nozzle allows the reservoir to be sealed off under vacuum before opening the chamber to air. The valve and

reservoir are wrapped in heater tape with the valve kept hotter than the cesium reservoir. During normal operations, the entire nozzle region is kept at a temperature of 170 °C while the cesium reservoir is kept at 110 °C. Higher temperatures produce a thermal Cs cloud which adds a nonlinear background to the fluorescence and transmission spectra. External to the nozzle array, we place a collimator constructed of #1 (0.170 × 25 × 25 mm) microscope cover slips with pieces of cover slips as spacers. The collimator restricts the velocity spread in the direction parallel to the laser beam, while allowing a reasonable part of the atomic beam to pass between the cover slips. The collimator geometrically restricts the atomic beam to a maximum possible full divergence angle of 13.6 mrad. Fitting the spectra indicates that the Doppler broadening due to beam divergence is 2.3(1) MHz which is consistent with our expectations based on the geometrical constraints of the collimator. Fig. 12 shows typical spectra of the $^{133}\text{Cs } 6s^2S_{1/2} F = 3 \rightarrow 6p^2P_{3/2} F' = 2, 3, 4$ and $6s^2S_{1/2} F = 4 \rightarrow 6p^2P_{3/2} F' = 5, 4, 3$ transitions (top graphs). The uncertainties in the fluorescence signal for each data point are given below the spectra. The frequency uncertainty for each data

point is between 5 and 25 kHz as shown on the bottom graphs.

6. Conclusions

Using the frequency calibration technique described in this paper, we were able to construct a diode laser based system for precision laser frequency measurements. The system uses heterodyning of two spectrally narrowed diode lasers. One laser serves as an optical frequency reference with a frequency stability of 30 kHz/h. Its linewidth is reduced with the help of an external Faraday filter cavity, and its frequency has been stabilized to the saturated absorption transitions in ^{133}Cs . The other laser can be scanned over a 500 MHz interval and is optically narrowed with an external confocal reflecting cavity. Both lasers have linewidths of the order of 50 kHz. The laser frequency difference is locked to a stable RF oscillator, and is scanned by scanning the RF frequency. The scanning laser excites a well-collimated thermal beam of Cs atoms. A specially constructed beam collimator reduces the thermal beam divergence to less than 13.6 mrad and provides a residual Doppler broadening of the spectra a factor of two less than the transition natural widths. A computer controls the RF oscillator frequency, and reads the corresponding laser frequency difference and thermal beam fluorescence signal. By keeping the RF oscillator frequency at specific values and averaging the measured fluorescence signal and the laser frequency difference, frequency calibrated spectra with better than 25 kHz resolution in each point and $S/N \sim 500$ are obtained.

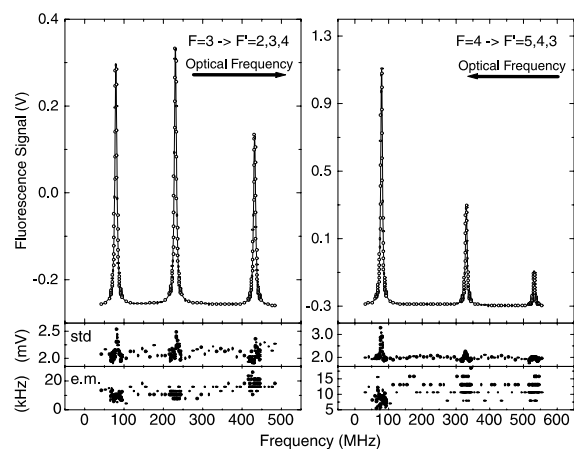


Fig. 12. Plot of the thermal beam fluorescence spectrum. The laser frequency difference is scanned by setting the RF oscillator at specific frequencies. The top trace is the averaged Cs fluorescence. The points are connected with a straight line. The second trace shows the fluorescence signal standard deviation (SD) for each data point. The bottom trace shows the frequency error in the mean (e.m.) for each data point.

Acknowledgements

We thank Steven Ruggiero, Leo Hollberg, and Jim Bergquist for their helpful discussions. Financial support for this work was provided by the Division of Chemical Sciences, Office of Basic Energy Sciences, Office of Energy Research at the US Department of Energy under Grant No. DE-FG02-95ER14579 and the Atomic and Molecular

Physics Program of the National Science Foundation under Grant No. PHY99-87984.

References

- [1] C.E. Tanner, C. Wieman, *Phys. Rev. A* 38 (3) (1988) 1616.
- [2] J. Lloyd Armstrong, in: *Theory of the Hyperfine Structure of Free Atoms*, first ed., Wiley-Interscience, John Wiley, New York, NY, 1971, p. 10016.
- [3] L. Young et al., *Phys. Rev. A* 50 (1994) 2174.
- [4] R.J. Rafac, C.E. Tanner, A.E. Livingston, H.G. Berry, *Phys. Rev. A* 60 (5) (1999) 3648.
- [5] R.J. Rafac, C.E. Tanner, *Phys. Rev. A* 58 (1998) 1087.
- [6] V. Gerginov et al., *Opt. Commun.* 187 (2001) 219.
- [7] W. Lee, J.C. Campbell, *Appl. Phys. Lett.* 58 (1991) 995.
- [8] Y. Shevy, J. Iannelli, J. Kitching, A. Yariv, *Opt. Lett.* 17 (1992) 661.
- [9] R.W. Drever et al., *Appl. Phys. B* 31 (1983) 97.
- [10] B. Dahmani, L. Hollberg, R. Drullinger, *Opt. Lett.* 12 (1987) 876.
- [11] A. Hemmerich et al., *Opt. Commun.* 75 (1990) 118.
- [12] H. Rong et al., *Opt. Commun.* 100 (1993) 268.
- [13] U. Schünemann et al., *Rev. Sci. Instrum.* 70 (1999) 242.
- [14] T. Udem, J. Reichert, R. Holzwarth, T.W. Hänsch, *Phys. Rev. Lett.* 82 (1999) 3568.
- [15] Defined by international agreement.